DOI 10.24425/pjvs.2021.136802

Original article

Interferon-γ-mediated gene expression in porcine alveolar macrophage; An *in vitro* model

Q. Liu, H.-Y. Wang

Nanchong Key Laboratory of Disease Prevention, Control, and Detection in Livestock and Poultry, Nanchong Vocational and Technical College, Nanchong 637131, China

Abstract

Alveolar macrophages (AMs) are not only important immune cell of the host, but also important target cell of a variety of respiratory pathogens. They play an important role in defense against pathogen invasion and in maintaining tissue balance. Interferon (IFN)-γ is a well known multipotent cytokine that has antiviral and antibacterial immune activity and enhances antigen presentation. To better reveal the biological processes of porcine AMs activated by IFN-γ, transcriptomic analysis was performed using Illumina HiSeq™ technique. The results identified 2,248 differentially expressed genes (DEGs), of which 753 were upregulated and 1,495 were downregulated, in porcine AMs 12 h after IFN-γ stimulation, compared with mock-treated porcine AMs. A gene ontology function enrichment analysis of these DEGs indicated that these genes were significantly enriched in functional clusters such as immune response, defense response, and intracellular signaling cascades. Analyzing the Kyoto Encyclopedia of Genes and Genomes pathways of the DEGs showed that these genes are mainly involved in cytokine–cytokine receptor interactions, alpha linolenic acid metabolism, and the RIG-I-like receptor signaling pathway. This study shows that a massive gene expression change occurred in porcine AMs following IFN-γ stimulation, which is critical for understanding the mechanisms of IFN-γ-mediated macrophage activation and immune regulation.

Keywords: pig; alveolar macrophage, IFN-γ, transcriptomic analysis

Introduction

Alveolar macrophages (AMs) are immune cells located in the interstitium of the lung, in the ducts below the bronchioles, and in the alveolar septa and cavities (Geissmann et al. 2010). They are derived from peripheral blood mononuclear cells, which originate from hematopoietic stem cells in the bone marrow (Joshi et al. 2018). On one hand, AMs play an important role in defense against invasion by exogenous pathogens (Medzhitov et al. 1997). When pathogens invade, AMs can respond directly by phagocytosis (Joshi et al. 2018). Meanwhile, AMs activate lymphocytes and other immune cells to achieve an immune defense response against the pathogens (Joshi et al. 2018). On the other hand, AMs are known to play an important

Correspondence to: Q. Liu, e-mail: liuqiang_yyy@163.com, tel.: +86-133-1461-1425

role in maintaining tissue balance (Labonte et al. 2014). Owing to their high heterogeneity and plasticity, they can present different degrees of proinflammatory or anti-inflammatory activities when stimulated by different endogenous or exogenous substances (Martinez et al. 2008). They regulate the inflammatory response process in lung tissues by secreting corresponding cytokines and chemokines and expressing different receptors and ligands (Martinez et al. 2008). Studies have shown that, when stimulated by different environments, they can be polarized into different subtypes, such as classically activated macrophages (M1) and alternatively activated macrophages (M2) (Mosser et al. 2008). At present, macrophages activated by classical and alternative pathways (Ml and M2) are considered the two extremes of the plasticity transition of macrophage function, and macrophages can switch between the two subtypes (Mosser et al. 2008). In response to bacterial and viral infections, the polarization of M1/M2 macrophages needs to be maintained in a controlled manner to effectively kill the pathogenic microorganisms without damaging the host (Porta et al. 2011). If excessive or persistent, M1-type polarization can kill invading pathogenic microorganisms, but it often also causes severe tissue damage (Porta et al. 2011). In contrast, if there are several M2-type macrophages and M1-type polarization is insufficient, killing the pathogenic microorganisms can be difficult and they may escape the host immune response (Porta et al. 2011). In addition, AMs are an important target for many viruses to infect, thereby escaping the antiviral immunity. A variety of respiratory-related pathogens, such as the porcine reproductive and respiratory syndrome virus (PRRSV) (Choi et al. 2002), porcine circovirus type 2 (Cheng et al. 2012), and classical swine fever virus(Li et al. 2020), can infect and proliferate in large numbers in AMs and are harmful to the porcine industry. Immunosuppression or immune damage caused by the destruction of AMs by pathogen infection is an important cause of damage, after which the pigs are prone to other pathogens, especially respiratory pathogenic microorganisms, which further aggravate the disease (Jung et al. 2009).

Interferon (IFN)-γ is a multifunctional cytokine, which can promote macrophage activation, mediate anti-virus and antibacterial immune responses, enhance antigen presentation, activate the innate immune system, coordinate the interaction between lymphocytes and endothelial cells, regulate the balance between T helper 1 and T helper 2 cells, and regulate cell proliferation and apoptosis (Polchert et al. 2008). IFN-γ is produced by T cells, natural killer cells, natural killer T cells, and antigen-presenting cells such as macrophages, dendritic cells (Frucht et al. 2001), and the Be-1 (Lund et al. 2010) and $CD11a^{hi}Fc\gamma RIII^{hi}$ subsets of B cells (Bao et al. 2014). This study uses Illumina HiSeq™ techniques to analyze transcriptome changes in IFN-γ-stimulated AMs, and to identify molecular changes in important pathways and their biological significance. This information is critical for understanding the mechanisms of IFN-γ-mediated macrophage activation and immune regulation.

Materials and Methods

Isolation and culture of porcine AMs

AMs isolation and culture have been described in previously published article (Liu et al. 2018). Briefly, three piglets were euthanized in the operation area of the pathoanatomy room (aseptic treatment). Under aseptic conditions, the lungs were removed and filled with RPMI1640 culture medium (containing 1% penicillin streptomycin mixture) (Gibco, Carlsbad, CA, USA). The collected liquid was resuspended in a 50 mL centrifuge tube (Corning, Ithaca, NY, USA) and centrifuged at 1,500 g for 10 min three times. The cell concentration was adjusted to 5.0×10^5 cells/mL. The AMs isolated from each pig were cultured separately in a 24-well plate (Corning) in an incubator (NuAire, MN, USA) with 5% CO_2, at 37°C. All animal experiments were approved by the Animal Protection and Utilization Committee of the Nanchong Vocational and Technical College.

Sample preparation, sequencing library preparation, sequencing data processing, and analysis

The AMs isolated from each pig were cultured separately for 24 h, and then stimulated with IFN-γ (100 ng/mL) (R&D systems, Minneapolis, USA). Culture medium was used as a negative control, in quadruplicate. After stimulation for 12 h, the control group cells from each pig were pooled and named A1, A2, and A3 for the three pigs, respectively; the cell samples of the corresponding IFN-γ treatment groups from each pig were also pooled, and named B1, B2, and B3 for three pigs, respectively. The control and treated cells were lysed using Trizol regent (Invitrogen, Carlsbad, CA, USA). The total RNA was extracted and purified. The mRNA was enriched with Oligo dT magnetic beads (Invitrogen), broken down into 200 nt fragments, and used as a template. The first strand of cDNA was synthesized using random six-base primers (Invitrogen), the second strand of cDNA was synthesized by adding buffer solution, dNTPs, RNaseH, and DNA polymerase I (Invitrogen) to complete the construction of the library. The sample was sequenced by the Shenzhen Huada company using HISSEQ™4000 (BGI Genomics

Table 1. Quality statistics of filtered reads and alignment results in the reference genome.

Sample	Total Raw Reads (M)[b]	Total Clean Reads (M)[c]	Total Clean Bases (Gb)[d]	Clean Reads Q20 (%)[e]	Clean Reads Q30 (%)[f]	Total Mapping Ratio (%)[g]	Unique Mapping Ratio (%)[h]
A1[a]	49.12	44.81	6.72	99.19	97.16	88.11	69.40
A2	49.12	44.57	6.68	99.19	97.14	84.05	66.62
A3	49.12	44.83	6.72	99.22	97.22	89.05	70.42
B1	49.12	44.60	6.69	99.19	97.15	87.92	68.82
B2	49.12	44.44	6.67	99.22	97.21	83.94	66.54
B3	49.12	44.64	6.70	99.23	97.30	89.72	70.16
Mean value	49.12	44.65	6.70	99.21	97.20	87.13	68.66

a: Sample name; b: Number of reads before filtration; c: Number of reads after filtration; d: Total base number after filtration; e: The ratio of base numbers with quality values greater than 20 to total base numbers in the filtered reads; f: The ratio of base numbers with quality values greater than 30 to total base numbers in the filtered reads; g: The ratio of clean reads aligned to the reference genome; h: The ratio of unique clean reads aligned to the reference genome.

Table 2. Statistics of genes and transcripts.

Sample	Total Gene Number	Known Gene Number	Novel Gene Number	Total Transcript Number	Known Transcript Number	Novel Transcript Number
A1	13,867	13,757	110	32,088	27,554	4,534
A2	13,207	13,089	118	30,907	26,512	4,395
A3	13,438	13,315	123	31,802	27,266	4,536
B1	13,091	12,982	109	30,698	26,289	4,409
B2	13,059	12,944	115	30,409	26,035	4,374
B3	13,296	13,177	119	31,530	27,038	4,492
Mean value	13,326	13,211	116	31,239	26,782	4,457

Company, Shenzhen City, China). The original data measured by Illumina HISSEQ™4000 were filtered, removing low quality reads and adaptors, and then compared with the reference genome using the transcriptome data comparison software TopHat2. Gene expression was calculated using the fragments per kilobase of transcript per million mapped reads method. The differentially expressed genes (DEGs) were analyzed by edgeR, screened using edgeR's general filtering standards (log2 |fold change| > 1 and false discovery rate < 0.05), and then analyzed for gene ontology (GO) and Kyoto Encyclopedia of Genes and Genomes (KEGG) enrichment. A hypergeometric test was used to identify the signaling pathways that were significantly enriched in the DEGs compared with the whole genome background. Signaling pathways with $p \leq 0.05$ were defined as being significantly enriched in the DEGs.

RT-qPCR

The total RNA of the cells was reverse transcribed into cDNA using random primer mix according to the instructions of the reverse transcription kit (Takara, Shiga, Japan). Relative fluorescence quantitative PCR was performed using TAKARA's SYBR Green qPCR Master Mix system (Takara) and an ABI7500 fluorescence quantitative PCR instrument (Stratagene, La Jolla, CA, USA). Glyceraldehyde-3--phosphate dehydrogenase was used as a reference gene. Four replicates were set up for each sample, as well as a blank control. The program included steps: 95°C for 60 s, followed by 95°C for 15 s, 60°C for 15 s, and 72°C for 45 s (40 cycles). A melting curve was determined. The ABI7500 data processing software was used to analyze and process the experimental data. The primers used are shown in Table 3. The fold changes of the target genes were evaluated using the $2^{-\Delta\Delta CT}$ relative expression analysis method (Abel et al. 2002).

Statistical analysis

Two-tailed Student's *t* test in GraphPad Prism (Version 7.02, GraphPad Software, San Diego, CA, USA) software was used for statistical analysis. A $p>0.05$ indicates that the difference is not significant, a $p<0.05$ indicates that the difference is significant; and a $p<0.01$ or $p<0.001$ indicates that the difference is extremely significant.

Table 3. Real-time PCR primers.

Gene Name	Primer sequence (5′→ **3′**)
CXCL9-F	5’ GAATGGACGTTGTTCCTGCAT 3’
CXCL9-R	5’ CCCCATTCTTCATTGTAGC 3’
CXCL10-F	5’ TCGCTGTACCTGCATCAAGAT 3’
CXCL10-R	5’ CATGTGGGCAAGATTGACT 3’
CXCL11-F	5’ AAGCAGTGAAAGTGGCAGATA 3’
CXCL11-R	5’ AGGCATCTTCGTCCTTTATGT 3’
RXFP1-F	5’ GGCAAGCATTATTCAGAGAGT 3’
RXFP1-R	5’ AAGGTCGCATACAGATGACA 3’
Loc106504234-F	5’ TGCCGTCTGCCTGTTCTATGG 3’
Loc106504234-R	5’ GGGCGGGCGTGACTACAGT 3’
CCL8-F	5’ TTCAGTCTCCATCCCGATCAC 3’
CCL8-R	5’ CGGCTTTGGTCTTGAAGATCA 3’
CSF1-F	5’ AACACTCCCAATGCCAACGTC 3’
CSF1-R	5’ GGCCTTGTCCTGCTCTTCGTA 3’
PSME2-F	5’ CCACCCAAGGATGATGAGATG 3’
PSME2-R	5’ GGCCAGGATCTTCTCGT 3’
C1QL2-F	5’ GTGCTCAAGTTCGACGACGTG 3’
C1QL2-R	5’ GCGCATGAGGATGTGGT 3’
DTX1-F	5’ TGTGCCGCAAGACCAAGAAGA 3’
DTX1-R	5’ ACCAGCCGCTCCATGCAG 3’
Loc102165146-F	5’ CTATATCCTTACGTGGCAAGA 3’
Loc102165146-R	5’ GAGGAGAGGGCTTGACTT 3’
GPR1-F	5’ CTTTGGCATCTGTTTGTGTAA 3’
GPR1-R	5’ CGGTACCGATGAGATAAGAC 3’
CCNB1-F	5’ CCCAAGAAGATGCTCCAAC 3’
CCNB1-R	5’ TGTCAGTCACAAAGGCAAAGT 3’
CCND2-F	5’ GAGTCCCAACTCCGAAGACCC 3’
CCND2-R	5’ TTCAACTTGCCCAGCACCAC 3’
LAMB1-F	5’ AATGTGACCGGTGTTTACCTG 3’
LAMB1-R	5’ TATGACCCGTGGTGTAGTCCT 3’
GADPH-F	5’ GTCATCCATGACAACTTCGG 3’
GADPH-R	5’ CACCAGTAGAAGCAGGGATG 3’

Results

Sequencing, data filtering, and reference genome alignment

The results showed a total of approximately 49 M reads for all libraries, with Q20≥99% and Q30≥97% (Table 1). The percentages of reads that matched the reference genome were 88.11%, 84.05%, 89.05%, 87.92%, 83.94%, and 89.72% in the A1, A2, A3, B1, B2, and B3 groups, respectively. The ratios of reads matching the unique reference genome were 69.40%, 66.62%, 70.42%, 68.82%, 66.54%, and 70.16%, respectively (Table 1). These uniform aligning rates indicate that the data are comparable between samples. The average total number of genes in all samples was 13,326, the average number of known genes was 13,211, the average number of predicted new genes was 116, and the average total number of transcripts detected in all samples was 31,239, of which 26,782 belonged to known protein coding genes (Table 2).

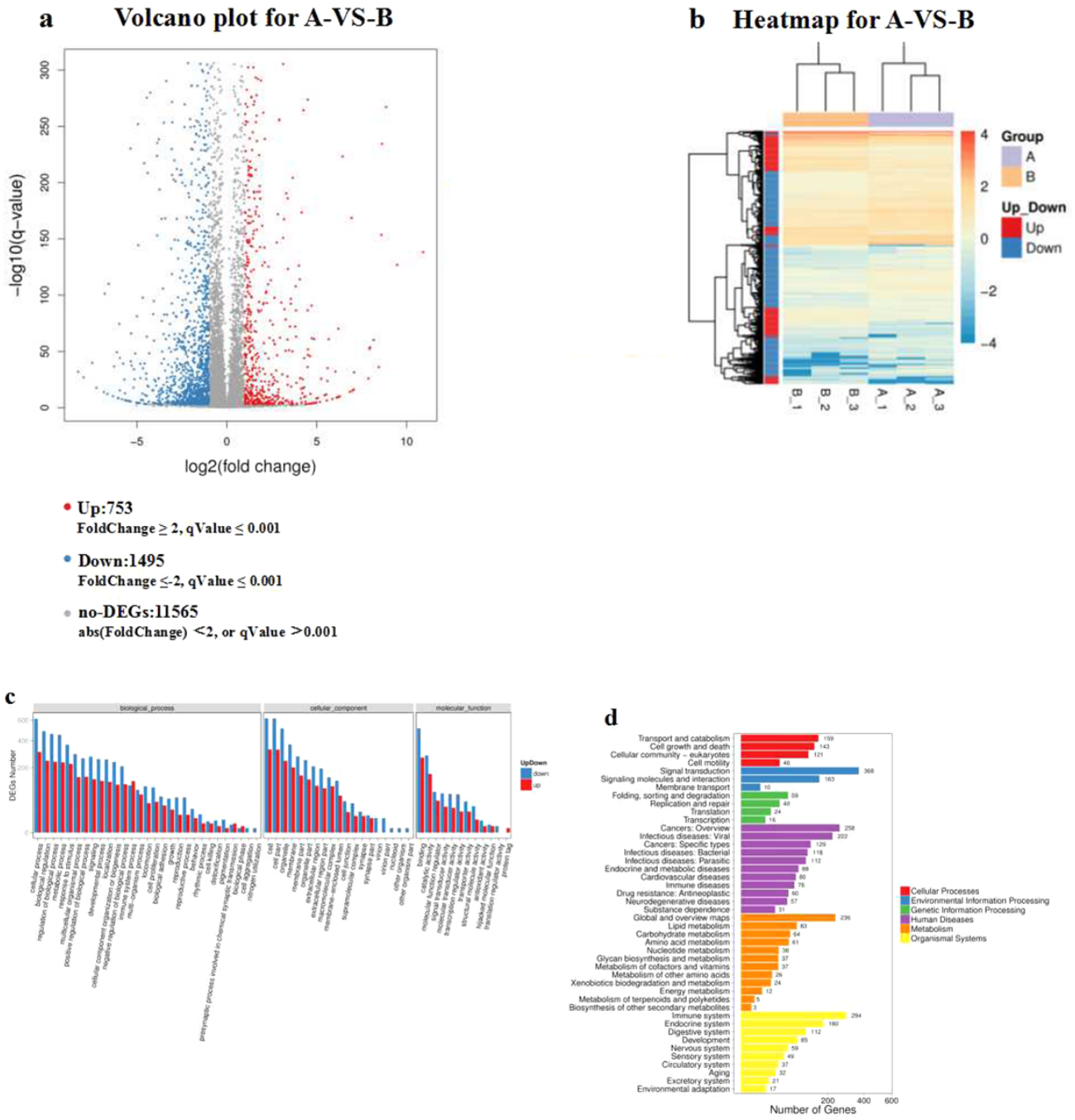

Fig. 1. Differential mRNA expression levels between IFN-γ-stimulated alveolar macrophages (AMs) and mock-treated AMs. (a) Volcano plot of differentially expressed genes (DEGs) in IFN-γ-stimulated AMs vs. mock-treated AMs. The x-axis represents the fold change of the DEGs, indicating log2 (fold change). The y-axis represents the significance of the DEGs, indicating -log10 (q value). (b) Heat map of DEGs in IFN-γ-stimulated AMs vs. mock-treated AMs. The rows represent the six samples for IFN-γ-stimulated (three samples, left) and mock-treated (three samples, right) AMs pooled from three individual pigs. On the y-axis, red indicates the upregulation and blue the downregulation of the genes. (c) Gene ontology (GO) enrichment analysis of the differentially expressed genes (DEGs). The lower x-axis shows the GO functions. The left y-axis shows the number of genes for each GO function. Red indicates the upregulation and blue the downregulation of genes. (d) Analysis of the Kyoto Encyclopedia of Genes and Genomes (KEGG) pathways of differentially expressed genes. Enriched pathways that meet the criteria of a q value ≤ 0.05 are defined as significantly enriched pathways. The x-axis shows the number of genes which belong to each specific KEGG pathways. The number of genes enriched in each pathway are shown at the top of each bar. The y-axis shows the KEGG pathways.

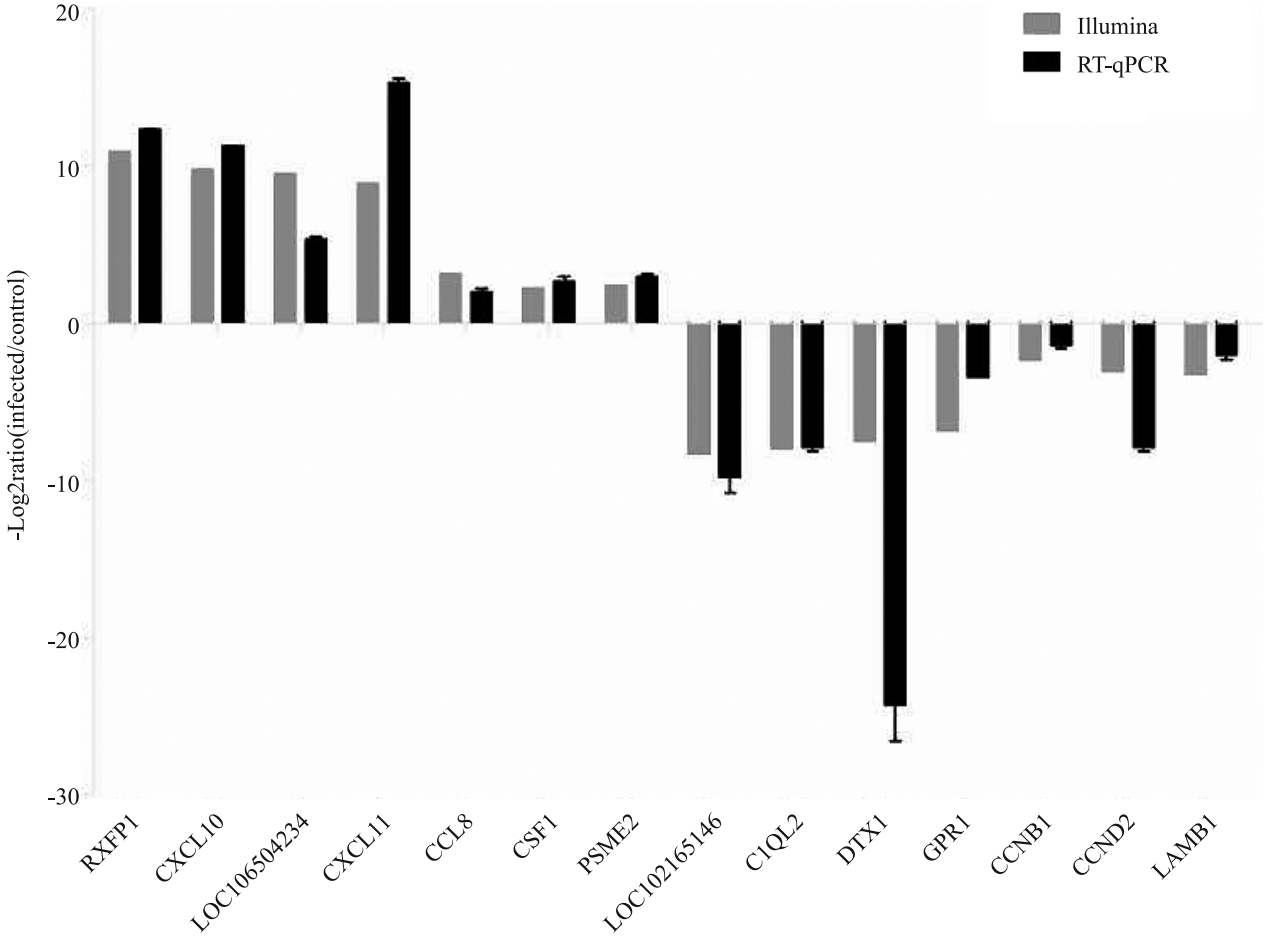

Fig. 2. Validation of Illumina sequencing data using RT-qPCR. The x-axis shows the gene symbol. The y-axis shows the log2 (ratio) relative expression value. Fold changes represent gene expression changes in IFN-γ-stimulated alveolar macrophages (AMs) relative to mock-treated AMs. Results are representative of three independent experiments. * $p<0.05$, ** $p<0.01$.

Analysis of difference in expression level of genes

In the treatment group, 2,248 DEGs were found compared with the control group. Among them, 753 genes were upregulated and 1,495 genes were downregulated (Fig. 1a). The scatter-plot shows the DEG distribution (Fig. 1a) and the heat map shows the evolutionary relationships between the samples (Fig. 1b).

GO function enrichment analysis of the DEGs

The results of the GO functional classification and enrichment analysis of the DEGs is shown in Fig. 1c. The GO enrichment results show that the top five significantly enriched major biological process categories were cellular process (924 DEGs/2,248 DEGs), biological regulation (733/2,248), regulation of biological process (701/2,248), metabolic process (689/2,248), and response to stimulus (591/2,248). In cell components, the top five enriched categories were cell (948/2,248), cell part (946/2,248), organelle (759/2,248), membrane (570/2,248), and membrane part (431/2,248). In molecular function, the top five enriched categories were binding (783/2,248), catalytic activity (445/2,248), molecular function regulator (127/2,248), signal transducer activity (105/2,248), and molecular transducer activity (100/2,248) (Fig. 1c).

KEGG enrichment analysis of the DEGs

The analysis results showed that the KEGG metabolic pathways in which the 1,260 DEGs are involved are mainly divided between six branches, and each branch has one most significant KEGG pathway, as shown in Fig. 1d. In the cellular processes pathways, the top three significantly enriched KEGG pathways were transport and catabolism (159 DEGs), cell growth and death (143), and cellular community-eukaryotes (121). In the environmental information processing pathways, the top three significantly enriched KEGG pathways were signal transduction (368), signaling molecules and infection (163), and membrane transport (10). In the genetic information processing pathways, the top three significantly enriched KEGG pathways were folding, sorting and degradation (59); replication

and repair (40); and translation (24). In the human disease (only animal) pathways, the top three significantly enriched KEGG pathways were cancers: overview (258), infectious diseases: viral (222), and cancers: specific types (129). In the metabolism pathways, the top three significantly enriched KEGG pathways were global and overview maps (236), lipid metabolism (83), and carbohydrate metabolism (64). Finally, in the organismal systems pathways, the top three significantly enriched KEGG pathways were immune system (294), endocrine system (180), and digestive system (112).

Validation of Illumina sequencing data using RT-qPCR

In this study, the top five upregulated and downregulated DEGs were selected and the results of Illumina sequencing were identified by RT-qPCR. The top five upregulated genes were relaxin family tide receptor 1, CXC motif chemokine (CXCL)10, Olfactory Loc 106504234, CXCL9, and CXCL11. The top five downregulated genes were Loc 102165146, complement C1q-like protein 2, e3 ubiquitin-protein ligase DTX1 isoform 2, GPN-loop GT2, and G-protein coupled receptor 1 isoform 1.

The RT-qPCR identification results are shown in the Fig. 2. Although there is a certain degree of difference in the values (only in fold change) measured by RT-qPCR and Illumina sequencing, the overall differential expression trends of the two methods are essentially the same. Therefore, the results of the Illumina sequencing are reliable.

Discussion

In this study, by transcriptomic sequencing of control and IFN-γ-treated AMs, we screened out the DEGs between the two groups. Through the GO and KEGG enrichment analyses of the DEGs, it was found that the molecules were significantly enriched in the signal transduction pathway, including the JAK–STAT signaling pathway, cytokine–cytokine receptor interactions, MAPK signaling pathway, and other signaling pathways belonging to the signal transduction pathway, and play an important role in molecular structure regulation, activity regulation, and protein expression (Schindler et al. 2007, Yeung et al. 2018). Through transcriptome analysis of the JAK–STAT signaling pathway, it was found that there are significantly upregulated molecules at the transcriptional level, including JAK2, STAT1, STAT2, suppressor of cytokine signaling 2, suppressor of cytokine signaling 3, and so on. The JAK–STAT signaling pathway is a cytokine-stimulated signal transduction pathway discovered in recent years (Schindler et al. 2007). It is involved in many important biological processes such as cell proliferation, differentiation, apoptosis, and immune regulation (Schindler et al. 2007). Several studies have shown that the JAK–STAT signaling pathways are activated during IFN-γ-mediated cell activation and are involved in the regulation of cellular polarization mechanisms (Su et al. 2015, Wang et al. 2018). Moreover, after IFN-γ stimulation of AMs, molecules such as CD40 molecule, chemokine (C-C motif) ligand 5, chemokine (C-C motif) ligand 10, fms-related tyrosine kinase 1, IL-1A, IL-7R, CXCR1, CXCR2, IL-12R, and IL-15 in the cytokine-cytokine receptor interaction receptor signaling pathways (e.g., the CC subfamily, CXC subfamily, interferon family, TNF family, and TGFβ family), and molecules such as Fas (TNF receptor superfamily, member 6), heat shock 70kDa protein 1-like, heat shock protein 70.2, and epidermal growth factor receptor, in the MAPK signaling pathway receptor signaling pathways, were significantly upregulated. Previous studies have shown that multiple monocyte/macrophage-tropic virus infections, such as PRRSV, can induce the expression of IFN-γ (Liu et al. 2017, Liu et al. 2018). Other studies suggest that immune response specific pathways, such as cytokine-cytokine receptor interactions and the JAK-STAT and MAPK signaling pathways, are activated by infections of immunosuppressive virus, such as PRRSV (Islam et al. 2016) and the swine influenza virus (Delgado-Ortega et al. 2014). It is speculated that these signaling pathways may also be involved in the regulation of the pathogenesis of viral infection.

This study found that the molecules in signaling pathways such as the Toll-like receptor (TLR) signaling pathway, RLR signaling pathway, NOD-like receptor (NLR) signaling pathway, and cytosolic DNA-sensing (CDS) pathway were significantly enriched. The TLR, RLR, NLR, and CDS signaling pathways belong to the pattern recognition receptor (PRR) signaling pathways and play a vital role in innate immune response (Fischer et al. 2018). It is suggested that IFN-γ stimulation can participate in immune regulation through the PRR signaling pathway. A complex interplay between macrophage activity and IFN-γ, through synergistic integrations of signals from other pathways involving PRRs, such as the TLR pathway, regulates the immune response cascade that is characterized by the transcriptional upregulation of many antiviral molecules, e.g., proinflammatory cytokines and IFN-stimulated genes (Fischer et al. 2018). In this study, we found that intrinsic antiviral factors, including members of GBP family, IFITMs family, TRIMs family, Tetherin/BST2, OASL, and SAMHD-1, were upregulated after stimulation (Supplementary Excel 1). These may be partially

related to IFN-γ-mediated antibacterial and antiviral immune response.

In addition, IFN-γ is a key cytokine that drives cellular immunity (Kang et al. 2018). IFN-γ plays an important role in immunoregulation by enhancing antigen processes and presentation (Kang et al. 2018). In this study, we found that CIITA, PSME2, RFX5, TAP2, TAP1, CD74, TAPBP, and B2M, which are related to antigen presentation, were significantly upregulated at the transcriptional level. According to Sautter et al., IFN-γ induces several antigen-presenting molecules, such as MHC-I, MHC-II, CD11a, and CD40 in monocyte-derived macrophages stimulated by IFN-γ alone or in combination with CSF-1/IFN-γ (Sautter et al. 2018). Mice devoid of IFN-γ genes or its receptors are highly susceptible to infectious pathogens and may die rapidly, which further highlights the importance of IFN-γ in antiviral cellular immunity (Kak et al. 2018).

Acknowledgements

This study was supported by grants from the Nanchong Vocational and Technical College for Basic Scientific Research (no. ZRA1904 and no. NZYBZ2002) and the Applied Technology Research and Development Programme of Nanchong (no. 19YFZJ0027).

References

Abel K, Alegria-Hartman MJ, Rothaeusler K, Marthas M, Miller CJ (**2002**) The relationship between simian immunodeficiency virus RNA levels and the mRNA levels of alpha/beta interferons (IFN-alpha/beta) and IFN-alpha/beta-inducible Mx in lymphoid tissues of rhesus macaques during acute and chronic infection. J Virol 76: 8433-8445.

Bao Y, Liu X, Han C, Xu S, Xie B, Zhang Q, Gu Y, Hou J, Qian L, Qian C, Han H, Cao X (**2014**) Identification of IFN-γ-producing innate B cells. Cell Res 24: 161-176.

Cheng S, Zhang M, Li W, Wang Y, Liu Y, He Q (**2012**) Proteomic analysis of porcine alveolar macrophages infected with porcine circovirus type 2. J Proteomics 75: 3258-3269.

Choi C, Cho WS, Kim B, Chae C (**2002**) Expression of interferon-gamma and tumour necrosis factor-alpha in pigs experimentally infected with Porcine Reproductive and Respiratory Syndrome Virus (PRRSV). J Comp Pathol 127: 106-113.

Delgado-Ortega M, Melo S, Punyadarsaniya D, Rame C, Olivier M, Soubieux D, Marc D, Simon G, Herrler G, Berri M, Dupont J, Meurens F (**2014**) Innate immune response to a H3N2 subtype swine influenza virus in newborn porcine trachea cells, alveolar macrophages, and precision-cut lung slices. Vet Res 45: 42.

Fischer S (**2018**) Pattern recognition receptors and control of innate immunity: role of nucleic acids. Curr Pharm Biotechnol 19: 1203-1209.

Frucht DM, Fukao T, Bogdan C, Schindler H, O'Shea JJ, Koyasu S (**2001**) IFN-gamma production by antigen-presenting cells: mechanisms emerge. Trends Immunol 22: 556-560.

Geissmann F, Manz MG, Jung S, Sieweke MH, Merad M, Ley K (**2010**) Development of monocytes, macrophages, and dendritic cells. Science 327: 656-661.

Islam MA, Grosse-Brinkhaus C, Proll MJ, Uddin MJ, Rony SA, Tesfaye D, Tholen E, Holker M, Schellander K, Neuhoff C (**2016**) Deciphering transcriptome profiles of peripheral blood mononuclear cells in response to PRRSV vaccination in pigs. BMC Genomics 17: 641.

Joshi N, Walter JM, Misharin AV (**2018**) Alveolar macrophages. Cell Immunol 330: 86-90.

Jung K, Renukaradhya GJ, Alekseev KP, Fang Y, Tang Y, Saif LJ (**2009**) Porcine reproductive and respiratory syndrome virus modifies innate immunity and alters disease outcome in pigs subsequently infected with porcine respiratory coronavirus: implications for respiratory viral co-infections. J Gen Virol 90: 2713-2723.

Kak G, Raza M, Tiwari BK (**2018**) Interferon-gamma (IFN-gamma): exploring its implications in infectious diseases. Biomol Concepts 9: 64-79.

Kang S, Brown HM, Hwang S (**2018**) Direct antiviral mechanisms of interferon-gamma. Immune Netw 18: e33.

Labonte AC, Tosello-Trampont AC, Hahn YS (**2014**) The role of macrophage polarization in infectious and inflammatory diseases. Mol Cells 37: 275-285.

Li C, Wang Y, Zheng H, Dong W, Lv H, Lin J, Guo K, Zhang Y (**2020**) Antiviral activity of ISG15 against classical swine fever virus replication in porcine alveolar macrophages via inhibition of autophagy by ISGylating BECN1. Vet Res 51: 22.

Liu Q, Zhang YL, Hu W, Hu SP, Zhang Z, Cai XH, He XJ (**2018**) Transcriptome of porcine alveolar macrophages activated by interferon-gamma and lipopolysaccharide. Biochem Biophys Res Commun 503: 2666-2672.

Liu Q, Zhang YL, Hu SP, Ma ZL, Gao SL, Sun B, Xiao F, Zhang Z, Cai XH, He XJ (**2017**) Expression of immunoproteasome subunits in the porcine lung: Alterations during normal and inflammatory conditions. Vet Microbiol 210: 134-141.

Lund FE, Randall TD (**2010**) Effector and regulatory B cells: modulators of CD4+ T cell immunity. Nat Rev Immunol 10: 236-247.

Martinez FO, Sica A, Mantovani A, Locati M (**2008**) Macrophage activation and polarization. Front Biosci 13: 453-461.

Medzhitov R, Janeway CA, Jr (**1997**) Innate immunity: impact on the adaptive immune response. Curr Opin Immunol 9: 4-9.

Mosser DM, Edwards JP (**2008**) Exploring the full spectrum of macrophage activation. Nat Rev Immunol 8: 958-969.

Polchert D, Sobinsky J, Douglas G, Kidd M, Moadsiri A, Reina E, Genrich K, Mehrotra S, Setty S, Smith B, Bartholomew A (**2008**) IFN-gamma activation of mesenchymal stem cells for treatment and prevention of graft versus host disease. Eur J Immunol 38: 1745-1755.

Porta C, Riboldi E, Totaro MG, Strauss L, Sica A, Mantovani A (**2011**) Macrophages in cancer and infectious diseases:

the 'good' and the 'bad'. Immunotherapy 3: 1185-1202.

Sautter CA, Auray G, Python S, Liniger M, Summerfield A (**2018**) Phenotypic and functional modulations of porcine macrophages by interferons and interleukin-4. Dev Comp Immunol 84: 181-192.

Schindler C, Levy DE, Decker T (**2007**) JAK-STAT signaling: from interferons to cytokines. J Biol Chem 282: 20059-20063.

Su X, Yu Y, Zhong Y, Giannopoulou EG, Hu X, Liu H, Cross JR, Ratsch G, Rice CM, Ivashkiv LB (**2015**) Interferon-gamma regulates cellular metabolism and mRNA translation to potentiate macrophage activation. Nat Immunol 16: 838-849.

Wang F, Zhang S, Jeon R, Vuckovic I, Jiang X, Lerman A, Folmes CD, Dzeja PD, Herrmann J (**2018**) Interferon gamma induces reversible metabolic reprogramming of M1 macrophages to sustain cell viability and pro-inflammatory activity. EBioMedicine 30: 303-316.

Yeung YT, Aziz F, Guerrero-Castilla A, Arguelles S (**2018**) Signaling pathways in inflammation and anti-inflammatory therapies. Curr Pharm Des 24: 1449-1484.